数理解析研究所講究録
1030巻 1998年 97-101

Gravity Waves Observed in a High-Resolution GCM Simulation

By

Kaoru Sato
Department of Geophysics, Faculty of Science, Kyoto University

Toshiro Kumakura
Department of Civil and Environmental Engineering, Nagaoka University of Technology

and

Masaaki Takahashi
Center for Climate System Research, University of Tokyo

1 Introduction

A lot of efforts have been made to elucidate gravity wave characteristics in the real atmosphere using various observational data. However, observational stations are not uniformly distributed on the earth and usually we cannot obtain all physical quantities from observations which are needed for the analysis. Thus, we use a GCM with high resolution both in the horizontal and vertical directions to examine global characteristics of gravity waves in the lower stratosphere.

2 Model Experiments

The model used is the first version of the atmospheric general circulation model (GCM) which was developed at the Center for Climate System Research / National Institute for Environmental Studies (CCSR/NIES) (Numaguti, 1993; Numaguti et al., 1995; Nakajima et al. (1995). The horizontal resolution is T106, which corresponds to a grid spacing of about 120 km. There are 53 layers in the vertical, having about 600 m vertical resolution in the upper troposphere and lower stratosphere. This fine vertical grid spacing is necessary to resolve small vertical wavelengths of gravity waves as observed in the real atmosphere. The top level of the model is located at about 0.5 hPa. The moist convective adjustment scheme is used as the cumulus parameterization in this experiment following Takahashi (1996) who successfully obtained realistic QBO in a GCM. The bottom boundary condition is that of an aqua-planet. Values of SST climatology in February are given independent of longitude and time (perpetual February). The other processes and schemes are almost the same as those in the standard GCM experiments. As for the start-up run, a horizontal resolution T21, 53 layers (T21L53) model of the same boundary condition was integrated with an initial condition of an isothermal atmosphere at rest over 120 model days to obtain a quasi-steady state. The final day of T21L53 model simulation was used as the initial condition of the T106L53 model. The T106L53 model was run for 80 days and obtained a quasi-steady state. The data of final 20 days at a time interval of 1 hour were used for the analysis of gravity wave activities. To avoid aliasing from fluctuations with higher frequencies, values averaged over one hour are used. As a result we obtained a realistic mean zonal wind

field. The subtropical westerly jet is situated around 32N and 45S, with peak values larger than 40 and 30 m s^{-1}, respectively. The polar night jet and subtropical jet are clearly separated in the northern hemisphere. The tropopause heights are also realistic; 15–16 km in the tropical region and about 9–10 km in the middle and high-latitude regions.

3 Comparison With MST Radar Observations

To see how realistic the gravity wave field simulated in this model is, we made comparison with observation data. Figure 1a shows a time-height section of meridional winds (v) obtained through a special long-term (19 days) continuous observation with the MU (Middle and Upper atmosphere) radar which is an MST radar located at Shigaraki, Japan (35N, 136E). See Fukao et al.(1985) for details of the MU radar. Clear downward propagating phase structure is observed in the height region of 19–25 km (see contours of 0 or 10 m s^{-1}), where the zonal mean wind is very weak. The vertical wavelength and wave period are about 3.5 km and 20 h, respectively. Sato et al. (1997) made detailed analysis and showed that the wave structure is due to inertia-gravity waves with a horizontal wavelength of about 1200 km propagating westward with a phase speed of about 10 m s^{-1}. The vertical and horizontal wavelengths are sufficiently large to be resolved in our high-resolution model.

Figure 1b shows a time-height section of simulated v at the latitude of 34.2N over 20 days. The tick marks on the right indicate the locations of vertical grids in the model. The tilt of zero contours of the simulated v (e.g., Day 10 and Day 16) is similar to that of radar observation (e.g., 12 and 20 April), indicating that simulated baroclinic waves are realistic. Most important is the feature that gravity wave structure having vertical wavelength and wave period similar to observation is seen in lower stratosphere in the model data. Comparison of power spectra indicates that the amplitude of simulated gravity waves accords with observation. This good agreement with observations suggests that the gravity wave field in our model is fairly realistic.

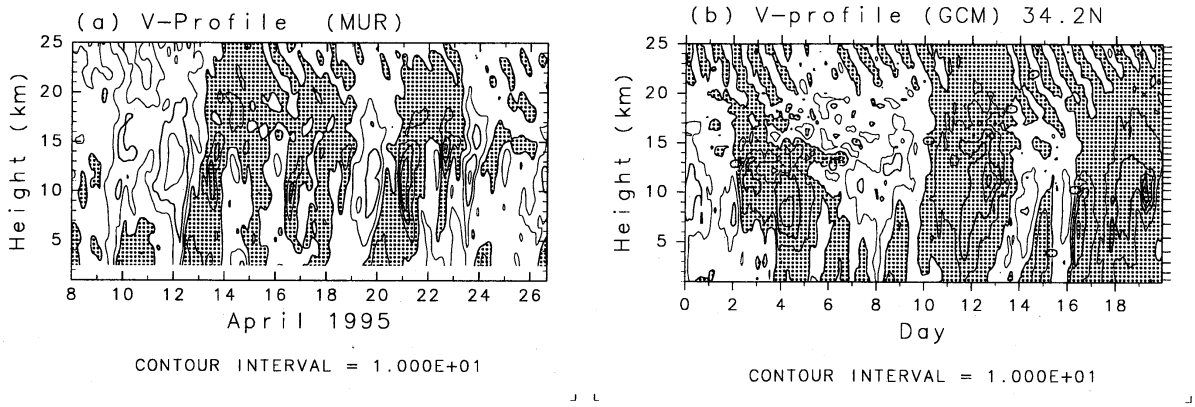

Fig. 1 Time-height sections of meridional wind (a) observed with the MU radar (35N, 136E) over 19 days in April, 1996 and (b) simulated by the GCM over 20 days (34.2N). Negative regions are darkly shaded. Contour intervals are 10 m s^{-1}.

4 Statistical Characteristics of Gravity Waves

Since there is no longitudinal dependence of boundary condition in the present model, the statistical characteristics of gravity waves must be independent of longitude. Thus, in the following sections we analyze time series of eight longitudes with the same longitudinal interval (45°) and examine the average as the statistics of the model.

4.1 Spectral characteristics as a function of latitude

Frequency power spectra were calculated at each of eight longitudes as a function of latitude (ϕ) and height (z), and the average of eight spectra was obtained. The spectra were further averaged for the the height regions of 22–27 km with fine vertical resolution. A result for v is shown in Fig. 2. Thick solid curves indicate the inertial frequency at each latitude and red dashed curves indicate the periods of one day and a half day.

Large values are distributed at higher frequency regions bordered with the curve of the inertial frequency. This is consistent with the theory of internal gravity waves that their wave frequencies should be higher than the inertial frequency. An interesting feature is that isolated peaks are observed around the inertial frequency at each latitude except around the equator. The spectra around the equator where the inertial frequency becomes zero are widely distributed and no particular peaks are observed.

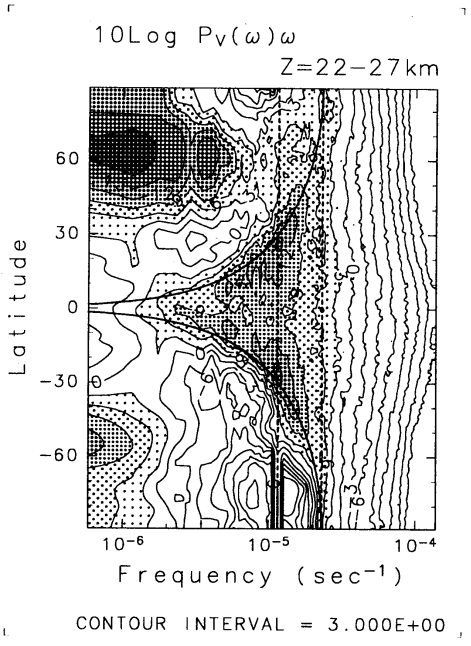

Fig. 2 Frequency power spectra in the energy-content form of v fluctuations simulated by GCM as a function of latitude for the height region of 22–27km. Contours are drawn for $10 \log P_v(\omega)\omega$ with intervals of 3dB. A thick solid curve indicates inertial frequency at each latitude. Two dashed lines indicate frequencies of 1 day and a half day.

4.2 Global energy distribution and meridional propagation of gravity waves

We made energy and momentum flux analysis for two kinds of components, which are frequently treated as gravity waves in observational studies: short-period (<1 day) waves and small vertical-scale (<5 km) waves. The momentum fluxes are useful values to examine the

horizontal propagation of internal gravity waves. Positive (negative) $\overline{u'w'}$ means eastward (westward) propagation and positive (negative) $\overline{v'w'}$ means northward (southward) propagation relative to the mean wind for gravity waves propagating energy upward. The signs are reversed for downward energy propagation. The vertical energy flux $\overline{p'w'}$, where p is the pressure, indicates dominance of upward energy propagation in the lower stratosphere for both two kinds of gravity wave components.

The distribution of $\overline{u'w'}$ shows the short-period gravity waves propagate westward relative to the mean wind (not shown). Interesting are the characteristics of $\overline{v'w'}$ (Fig. 3a). Negative (positive) values are observed in the southern (northern) hemisphere. Moreover the latitudinal expanse of large $\overline{v'w'}$ increases as altitude increases. The edge of the large $\overline{v'w'}$ region reaches the mid-latitude of ϕ =50° at z =27 km. This V-shaped distribution suggests that gravity waves are generated in the equatorial region and propagate poleward in both hemispheres.

The energy and momentum flux features of small vertical-scale waves are similar to those of short period waves: wave energy is maximized around the equator; the waves propagate westward relative to the mean wind. However there are a few remarkable differences. Figure 3b shows latitude-height sections of $\overline{v'w'}$ for small vertical-scale waves. It is noted that negative (positive) values of $\overline{v'w'}$ above the subtropical jet in the northern (southern) hemisphere. This means equatorward propagation of gravity waves and is consistent with observations (Sato, 1994). This feature is not seen for short-period waves. Thus small vertical-scale waves propagating equatorward above the subtropical jet have wave periods longer than 1 day. The $\overline{v'w'}$ profile in the equatorial region suggests the dominance of poleward propagation from the equator, similar to short-period waves, but the magnitude is smaller. Thus short-period waves propagating poleward have vertical wavelengths longer than 5 km.

A westward force calculated from the Eliassen-Palm flux due to gravity waves was 5 m s^{-1} $month^{-1}$ at the maximum in the upper part of the subtropical westerly jet around 30N, which is smaller by one order of magnitude compared with the drag due to topographically forced gravity waves (e.g. Palmer et al., 1986; McFarlane, 1987).

5 Concluding Remarks

With the aid of a high-resolution GCM (T106L53), global distribution and characteristics of gravity waves were examined. By using subsets out of the huge amount of data obtained with this high-resolution GCM simulation like observational data, further interesting analyses are possible: three dimensional structure of gravity waves having near-inertial frequency in the stratosphere; the generation and interaction with synoptic-scale baroclinic waves of gravity waves that are dominant above the subtropical jet; and the possible role of small-scale gravity waves on the QBO in the equatorial stratosphere. However, it is a matter of course, and we have to keep it in mind that observation and model studies are complementary.

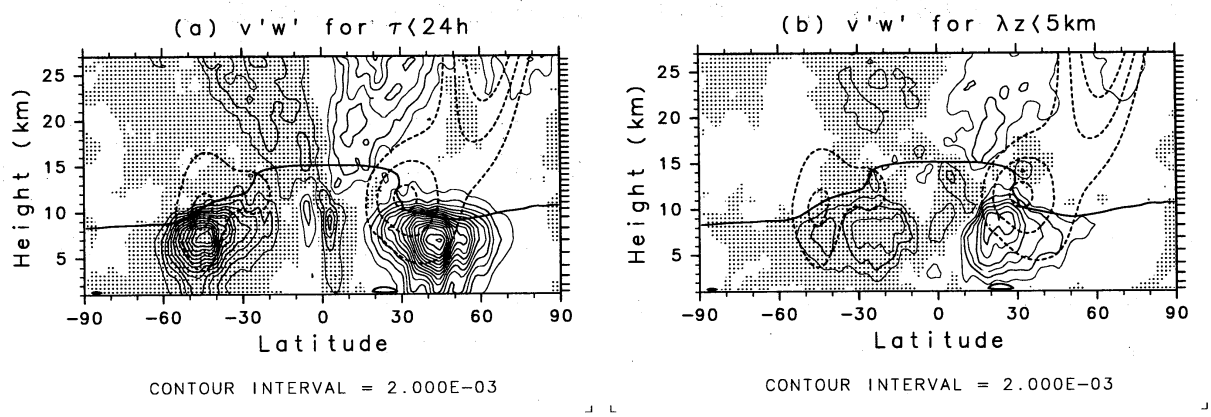

Fig. 3 Latitude-height sections of vertical fluxes of meridional momentum ($\overline{v'w'}$) for (a) short-period gravity waves and (b) small vertical-scale waves. Contour intervals are 0.002 m^2 s^{-2}. Negative regions are shaded.

Acknowledgment

This study was supported by Center for Climate System Research of the University of Tokyo, partly by a Grant-in-Aid for Scientific Research (A) (2)08404026 (KS) and (B) 06452083 (MT) of the Ministry of Education, Science and Culture, Japan, and by International Cooperative Study of Stratospheric Change and its Role in Climate from the Science and Technology Agency of Japan (TK). A part of calculation of the low resolution model was made by KDK (Kyoto daigaku Denpakagaku Keisanki-jikken souchi) Radio Atmospheric Science Center (RASC) of Kyoto University. The MU radar belongs to and is operated by RASC of Kyoto University. GFD-DENNOU library were used for drawing figures. This paper was submitted to J. Atmos. Sci.

REFERENCES

1. Fukao, S., T. Sato, T. Tsuda, S. Kato, K. Wakasugi and T. Makihira, 1985:*Radio Sci.*, **20,** 1155–1168.
2. McFarlane, N.A., 1987: *J. Atmos. Sci.*, **44,** 1775–1880.
3. Nakajima, T., M. Tsukamoto, Y. Tsusima, and A. Numaguti, 1995: *Studies of global environment change with special reference to Asia and Pacific regions,* **I-3,** 104-123.
4. Numaguti, A., M. Takahashi, T. Nakajima, and A. Sumi, 1995: *ibid,* **I-3,** 1-27.
5. Numaguti, A., 1993: *J. Atmos. Sci.*, **50,** 1874-1887.
6. Palmer, T.N., G.J. Shutts, and R. Swinbank, 1986: *Quart. J. Roy. Met. Soc.*, **112,** 1001–1040.
7. Sato, K., 1994: *J. Atmos. Terr. Phys.*, **56,** 755–774.
8. Sato, K., D. J. O'Sullivan and T. J. Dunkerton, 1997: *Geophys. Res. Lett.*, **24,** 1739–1742.
9. Takahashi, M., 1996: *Geophys. Res. Let.*, **23,** 661-664.